Convergence and numerics of a multi-section method for scattering by three-dimensional rough surfaces

Eric Heinemeyer [1], Marko Lindner and Roland Potthast [2]

October 25, 2006

Abstract

We introduce a novel *multi-section method* for the solution of integral equations on unbounded domains. The method is applied to the rough-surface scattering problem in three dimensions, in particular to a Brakhage-Werner type integral equation for acoustic scattering by an unbounded rough surface with Dirichlet boundary condition, where the fundamental solution is replaced by some appropriate half-space Green's function.

The basic idea of the multi-section method is to solve an integral equation $A\phi = f$ by *approximately* solving the equation $P\,AP_\tau\phi = P\,f$ for some positive constants $,\tau$. Here P is a projection operator that truncates a function to a ball with radius > 0. For a very general class of operators A, for which the Brakhage Werner equation from acoustic scattering is a particular example, we will show existence of approximate solutions to the multi-section equation and that approximate solutions to the multi-section equation approximate the true solution ϕ_0 of the operator equation $A\phi = f$. Finally, we describe a numerical implementation of the multi-section algorithm and provide numerical examples for the case of rough surface scattering in three dimensions.

1 IntrF3rpd

Model Problem. The basic model problem for our work is the solution of integral equations over unbounded domains which appear in what is usually called the *rough surface scattering problem*

The operator P truncates a function on $\mathbb{R}^2$ to its values inside the disk

(6) $$B := \{x \quad \mathbb{R}^2 : |x| < \quad \}.$$

In these notations $|\cdot|$ denotes an arbitrary norm in $\mathbb{R}^2$. In particular, in our numerical part in Section 4 we will use the maximum norm $|x| := \max(|x$

2 Scattering by rough surfaces

We restrict our attention to time-harmonic acoustic waves, which are modelled by the *Helmholtz equation*

$$\Delta u + \kappa^2 u = 0. \tag{11}$$

Here, κ denotes the wave number, which for the real-valued case is linked to the speed of sound c and the frequency ω via $\kappa = \omega/c > 0$. Often, κ is admitted to be a complex number $\kappa = \kappa_0 + i\sigma$, where the imaginary part σ models the properties of some lossy medium.

For our scattering surface Γ we assume that $f \in BC^{1,\alpha}(\mathbb{R}^2)$ for some $\alpha \in (0, 1]$. Further, f is assumed to satisfy the bounds

$$0 < f^- \le f(x) \le f^+, \quad x \in \mathbb{R}^2. \tag{12}$$

We consider the scattering of an *incident acoustic wave* u^i by the surface Γ. The *total field* $u := u^i + u^s$ is the sum of the incident field and the *scattered field* u^s. The scattered field is a solution to the Helmholtz equation (11) in D. Further, we assume that u satisfies the *Dirichlet boundary condition*

$$u \tag{13}$$

A solution to the boundary value problem can be found via the single- and double-layer potential approach. We define the *single-layer potential*

$$u_1(x) = \int_\Gamma G(x,y)\phi(y)\, ds(y), \quad x \in \mathbb{R}^3, \tag{23}$$

and the *double-layer potential*

$$u_2(x) = \int_\Gamma \frac{\partial G(x,y)}{\partial \nu(y)}\phi(y)\, ds(y), \quad x \in \mathbb{R}^3. \tag{24}$$

The boundary values of these potentials can be calculated using the boundary integral operators S and K defined by

$$(S\phi)(x) = 2\int_\Gamma G(x,y)\phi(y)\, ds(y), \quad x \in \Gamma, \tag{25}$$

and the *double-layer potential*

$$(K\phi)(x) = 2\int_\Gamma \frac{\partial G(x,y)}{\partial \nu(y)}\phi(y)\, ds(y), \quad x \in \Gamma. \tag{26}$$

It is shown in [1] that the combined single- and double layer potential

$$v(x) := u_2(x) - i\eta u_1(x), \quad x \in D, \tag{27}$$

with parameter $\eta > 0$ satisfies the boundary value problem (21) if and only if the density $\phi \in L^2(\Gamma)$ satisfies the integral equation

$$(I + K - i\eta S)\phi = 2g, \tag{28}$$

which is of the form $(I - W)\phi = f$ with $W = -K + i\eta S$ and $f = 2g$. The basic uniqueness and existence result is given by Theorem 3.4 of [2] as follows.

Theorem 2.2. *The operator $I + K - i\eta S$ is boundedly invertible on $L^2(\Gamma)$, and for the norm of its inverse, one has*

$$\|(I + K - i\eta S)^{-1}\| \le B, \tag{29}$$

where the constant B, as given in (3.4) in [2], only depends on the quotient κ/η and the Lipschitz constant of f.

As a result of Theorem 2.2 we obtain the existence of the solution for the rough surface scattering problem. In principle, the solution to the scattering problem is given by the combined potential (27) with a density ϕ which satisfies (28). Our main topic here is the numerical solution of such integral equations in three dimensions. We need to treat the numerical integration of functions over unbounded surfaces.

3 The multi-section method (MSM)

We will formulate our multi-section method for the following abstract setting which includes the rough surface scattering problems discussed above.

Let Y be a Banach space, and let $\{P_\tau\}_{\tau>0}$ be a family of linear operators on Y with the following three properties,

(P1) $P_\sigma P_\tau = P_\tau = P_\tau P_\sigma$ for all $\sigma \geq \tau > 0$,
(P2) $\|P_\tau\| = 1$ for all $\tau > 0$,
(P3) $P_\tau \to I$, that means $P_\tau \phi \to \phi$ for all $\phi \in Y$, as $\tau \to \infty$.

From (P1) with $\sigma = \tau$ we get that every P_τ is a projection operator. We will also have to deal with the complementary projectors $I - P_\tau$ which, for brevity, shall be denoted by Q_τ, for every $\tau > 0$.

Now suppose A is a bounded linear operator on Y with

(A1) A is invertible (and therefore boundedly invertible) on Y,
(A2) $Q_\sigma A P_\tau \to 0$ as $\sigma \to \infty$ for every fixed $\tau > 0$.

For illustration we give an example of Y, $\{P_\tau$

$$= \left(\int_{r=\varepsilon}^{+\infty} \frac{1}{r^{\gamma p}} |\partial B_r| \, dr \right) |B_\tau|^{p/q} 2^{\gamma p} C^p$$

$$= \left(\int_{r=\varepsilon}^{+\infty} \frac{r^{n-1}}{r^{\gamma p}} \, dr \right) |\partial B_1| |B_\tau|^{p/q} 2^{\gamma p} C^p$$

$$= \varepsilon^{n-\gamma p} \frac{1}{\gamma p - n} |\partial B_1| |B_\tau|^{p/q} 2^{\gamma p} C^p. \tag{33}$$

Finally, taking p-th roots proves (32). The proof for $p = 1$ is similar. But instead of using Hölder's inequality one immediately arrives at (33), with p/q replaced by 0. □

We illustrate the generality of our approach with three more examples of Banach spaces Y with projections P_ε and operators A acting on them.

Example 3.3. *Let* $Y = \ell^p(\mathbb{Z}^n)$ *with* $1 \le p < \infty$ *and* $n \in \mathbb{N}$. *Define* P_ε*, with* $\varepsilon > 0$, *literally as in (5) but with* $x \in \mathbb{Z}^n$*, of course. Also here, (P1)–(P3) clearly hold.*

In this case, in fact every bounded linear operator A *on* Y *is subject to (A2)! This can be seen as follows. Since all* P_τ *are compact operators on* Y*, also* AP_τ *is compact for every* $\tau > 0$. *But since, by (P3),* $Q_\varepsilon \to 0$ *as* $\varepsilon \to \infty$*, and since point-wise convergence on compact sets is uniformly, we get that even (A2) holds.*

Example 3.4. *Let* $Y = C[0,1]$. *For* $m \in \mathbb{N}$*, let* $P_m\phi$ *denote the piece-wise linear function which interpolates* $\phi \in Y$ *at the points* $j/2^m$ *with* $j = 0, \dots, 2^m$*, and for arbitrary* $\varepsilon > 0$*, put* $P_\varepsilon = P_{[\varepsilon]}$ *with* $[\varepsilon]$ *denoting the integer part of* ε. *Then it is easy to see that (P1)–(P3) are fulfilled.*

Example 3.5. *Let* $Y = L^2(\mathbb{T})$ *where* $\mathbb{T} := \{z \in \mathbb{C} : |z| = 1\}$ *is the complex unit circle. For* $m \in \mathbb{N}$*, let*

$$(P_m\phi)(t) = \sum_{k=-m}^{m} \text{[illegible]}$$

element $f \quad Y$, we are looking for the (unique) solution $\phi =: \phi_0$ of (1); that is

$$A\phi = f.$$

For the approximof23.87-21.-2602

Lemma 3.9. *Let $\tau_0 > 0$ be an admissible τ-bound for a given precision $\delta > 0$. If $\tau > \tau_0$ and $\quad > 0$ are such that $Q\,AP_\tau \quad < 1/\,A^{-1}$, then the set of all solutions of (MSM) is a bounded subset of Y. Precisely, every solution $\phi \quad Y$ of the system (MSM) is subject to $\phi \;_Y \le M$ with M given by (36).*

Proof. Suppose $\phi \quad Y$ solves (MSM) for given parameters $\delta,\ ,\tau > 0$. Then

$$\begin{aligned} A\phi \;-\; P\,f \quad &\le \quad A\phi - P\,f \quad = \quad AP_\tau\phi - P\,f \\ &\le \quad AP_\tau\phi - P\,AP_\tau\phi \;+\; P\,AP_\tau\phi - P\,f \\ &\le \quad Q\,AP_\tau \;\cdot\; \phi \;+\delta \end{aligned}$$

together with $\phi \;\le\; A^{-1} \;\cdot\; A\phi$ implies that

$$\begin{aligned} \frac{\phi}{A^{-1}} \;\le\; A\phi \quad &\le \quad P\,f \;+\; Q\,AP_\tau \;\cdot\; \phi \;+\delta \\ &\le \quad f \;+\; Q\,AP_\tau \;\cdot\; \phi \;+\delta \end{aligned}$$

and hence

$$\phi \;\le\; M \;:=\; \frac{f \;+\; \delta}{\qquad} \tag{36}$$

Now let $\phi \quad Y$ be a solution of (MSM) with parameters δ, τ and as chosen above. From (38) we get $Q\ AP_\tau \ < 1/\ A^{-1}$, and hence, by Lemma 3.9,

$$\phi \quad \leq M \tag{39}$$

with M as defined in (36). Moreover, inequality (38) is equivalent to

$$Q\ AP_\tau \quad < \ \frac{1}{A^{-1}} \cdot \frac{\frac{\varepsilon}{3(\ f\ +\delta)\cdot\ A^{-1}}}{1+\frac{\varepsilon}{3(\ f\ +\delta)\cdot\ A^{-1}}},$$

and hence to

$$\left(1+\frac{\varepsilon}{3(\ f\ +\delta)\cdot\ A^{-1}}\right)\cdot\ Q\ AP_\tau \quad < \ \frac{1}{A^{-1}} \cdot \frac{\varepsilon}{3(\ f\ +\delta)\cdot\ A^{-1}}.$$

This, moreover, is equivalent to

$$\begin{aligned} Q\ AP_\tau \quad &< \ \frac{1}{A^{-1}} \cdot \frac{\varepsilon}{3(\ f\ +\delta)\cdot\ A^{-1}} - \frac{\varepsilon}{3(\ f\ +\delta)\cdot\ A^{-1}} \cdot\ Q\ AP_\tau \\ &= \ \frac{\varepsilon(1/\ A^{-1}\ -\ Q\ AP_\tau\ )}{3(\ f\ +\delta)\cdot\ A^{-1}} \ = \ \frac{\varepsilon}{3M\ A^{-1}} \end{aligned} \tag{40}$$

with M as defined in (36). Then we have

$$\begin{aligned} \phi - \phi_0 \quad &= \quad P_\tau\phi - \phi_0 \quad = \quad A^{-1}AP_\tau\phi - A^{-1}f \quad \leq \quad A^{-1}\ \cdot\ AP_\tau\phi - f \\ &\leq \quad A^{-1}\ \cdot\ AP_\tau\phi - P\ AP_\tau\phi \quad + \quad P\ AP_\tau\phi - P\ f \quad + \quad P\ f - f \\ &\leq \quad A^{-1}\ \cdot\ Q\ AP_\tau\ \cdot\ \phi \quad + \ \delta \ + \quad Q\ f \\ &\leq \quad \frac{\varepsilon}{3} + \frac{\varepsilon}{3} + \frac{\varepsilon}{3} = \varepsilon, \end{aligned}$$

using inequalities (40) and (39) and the bounds on δ and $Q\ f$ in the last step. □

Remark 3.11. *One way to e ectively solve the system (MSM) for given parameters , τ and δ is to compute a $\phi \quad Y$ that minimizes the discrepancy in (8), for example using a gradient method or, if possible, by directly applying the Moore Penrose pseudo-inverse $B^\dagger$ of $B\ P\ f \quad \phi_0$ +the*

However, if is su ciently large, then, by (A2) and (P3), the equation (41) is just a small perturbation of

$$P_\tau A\ AP_\tau \phi \ = \ P_\tau A\ f, \tag{42}$$

which is nothing but the finite section method for the equation

$$A\ A\phi \ = \ A\ f. \tag{43}$$

Note that the finite section method (42) is applicable since A A is positive definite (see, e.g. Theorem 1.10 b in [5]). Clearly, if A is invertible, as we require in (A1), then also its adjoint A is invertible, and (43) is equivalent to our original equation (1).

Summarizing, if Y is a Hilbert space and all P are self-adjoint, then minimizing $P\ AP_\tau \phi - P\ f$ *is equivalent to solving a slight perturbation (41) of the finite section method (42) for (43).*

The multi-section method can be applied to the rough surface scattering problem of Section 2, as we know from Example 3.1, Lemma 3.2 and inequalities (18) and (19). In particular, note that the bound (29) on A^{-1} enables us to actually compute the corresponding terms in step (a) and (c) in the proof of Theorem 3.10.

We summarize the results in the following theorem.

Theorem 3.12 (MSM for rough surface scattering). *The multi-section method as defined in Definition 3.6, applied to rough surface scattering (11), (13), (14) and (15), is convergent in the sense of Theorem 3.10.*

4 Numerical realization and examples

The goal of this final section is to provide a numerical algorithm for the solution of the integral equation (28) using the multi-section method. For simplicity, we employ a low-order scheme for the treatment of the singularity of the operator, leaving more sophisticated high-order approaches to [6].

Our numerical approach to the solution of the system (MSM) for the concrete operator equation (28) is to choose some large parameters and τ and to choose the discrepancy δ as small as it possibly can be by looking for a function $\phi \quad L^2(B_\tau)$ that minimizes the MSM-residual $P\ AP_\tau \phi - P\ f$.

We have implemented both a *direct solver* for the minimization of the corresponding MSM-residual and an *iterative scheme* based on a gradient method. In

both cases we first transform the truncated approximate equation (8) into a matrix equation which, for simplicity, we denote by

$$A\phi = b. \tag{44}$$

The direct solver then approximately solves this equation via the Moore-Penrose pseudo inverse $A^{\dagger}$ of A. Precisely,

$$\phi = A^{\dagger} \circ b \tag{45}$$

has the smallest norm among all ϕ that minimize the residual $\|A\phi - b\|$.

This scheme is rather quick, but limits the number of unknowns N to several thousands, since we need to store fully occupied matrices of size N^2. This leads to a bound of approximately 10 on the number of wavelengths which can be resolved, since, for example, $N = 2500$ unknowns correspond to a grid-size of 50×50 grid points on our surface, and we need at least 5 points per wavelength for its resolution.

For problems with more unknowns we used an iterative solver, where the func-

For the iteration scheme the computation time per iteration scales quadratically in the number of unknowns. If we want to keep the time for one gradient step in the time-frame of hours, this limits the size of the problem to approximately $N = 100.000$, which corresponds to a grid of 350×350 or a resolution of 70 wavelengths. It is clear that at this point matrix compression schemes like the fast multipole method need to be employed. Since our main point here is the presentation of the multi-section method and the proof of its applicability we leave this to future research.

The main ingredient of equation (28) is the integral operator $I + K - i\eta S$, which, for the MSM, is applied to some density $P_\tau \phi$ supported on B_τ

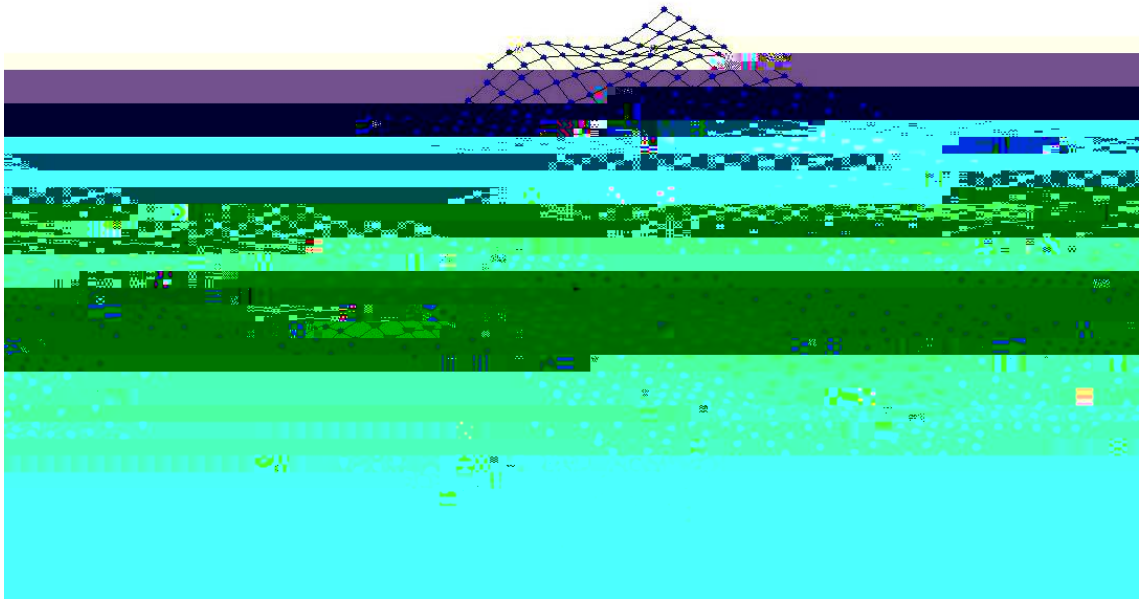

Figure 1: Setting for the multi-section method. The set B is shown with blue dots, the set B_τ with red triangles.

with

$$A = (I - W) \circ P_\tau , \tag{58}$$

$$\phi = \begin{pmatrix} \phi(x_1) \\ \vdots \\ \phi(x_M) \end{pmatrix}, \tag{59}$$

$$f = \begin{pmatrix} f(x_1) \\ \vdots \\ f(x_M) \end{pmatrix}, \tag{60}$$

$$W = \begin{pmatrix} \alpha_1 k(x_1, x_1) & \dots & \alpha_M k(x_1, x_M) \\ \vdots & & \vdots \\ \alpha_1 k(x_M, x_1) & \dots & \alpha_M k(x_M, x_M) \end{pmatrix}, \tag{61}$$

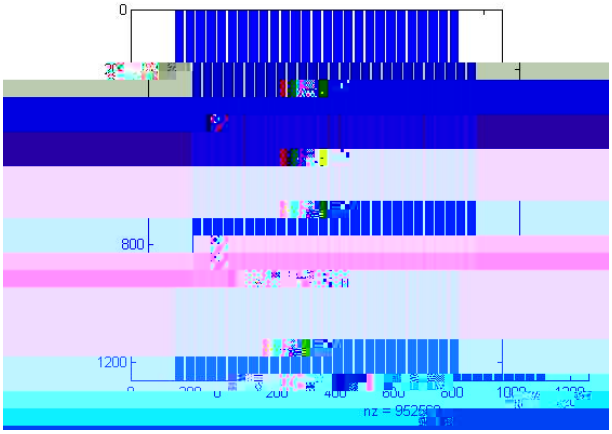

Figure 2: Structure of the matrix $A = (I - W) \circ P_\tau$.

and the projector P_τ is defined by

$$P_\tau = \mathrm{diag}(v), \quad v_j = \begin{cases} 1, & \text{if } x_j \in B_\tau \\ 0, & \text{otherwise,} \end{cases} \tag{62}$$

for $j = 1, \ldots, M$.

The solution of (57) is calculated using the Moore-Penrose pseudo inverse $A^\dagger$ (in Matlab realized via the function pinv(A)) applied to f, i.e. via

$$\phi_{\mathrm{sol}} := \left((I - W) \circ P_\tau \right)^\dagger f. \tag{63}$$

As a test example for the numerical realization of the multisection method we use the surface Γ defined by

$$f(x_1, x_2) := c_0 \cdot \sin(x_1) \cdot \cos(x_2) + 2$$

with $c_0 = 1/2$. Here, we place the source point z of the incident point-source $\Phi(\cdot, z)$ below the surface Γ, but above the plane $x_3 = 0$. In this case the scattered field is given by $-\Phi(\cdot, z)$. Thus, we can test the precision of the combined single- and double-layer potential with density ϕ calculated via the multi-section method.

Figure 3 (a) shows the original fields for an incident point source with source point $(-2, 0, 0.2)$. The reconstructed field is shown in Figure 3 (b). Here, we worked with the direct method and employed the multi-section method with $= 3\pi$ and $\tau = 0.8$. The figures show a grid of 40 × 40 points.

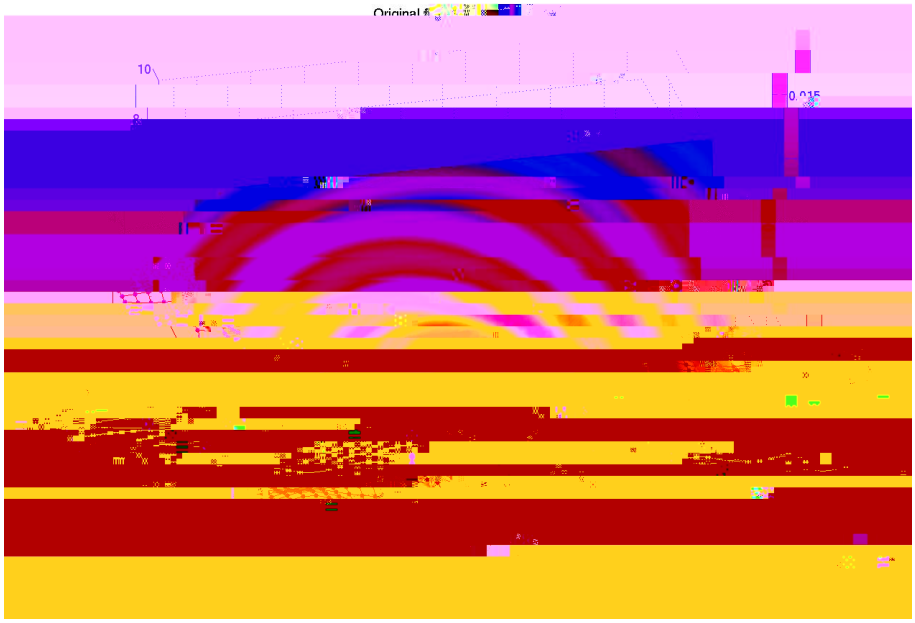

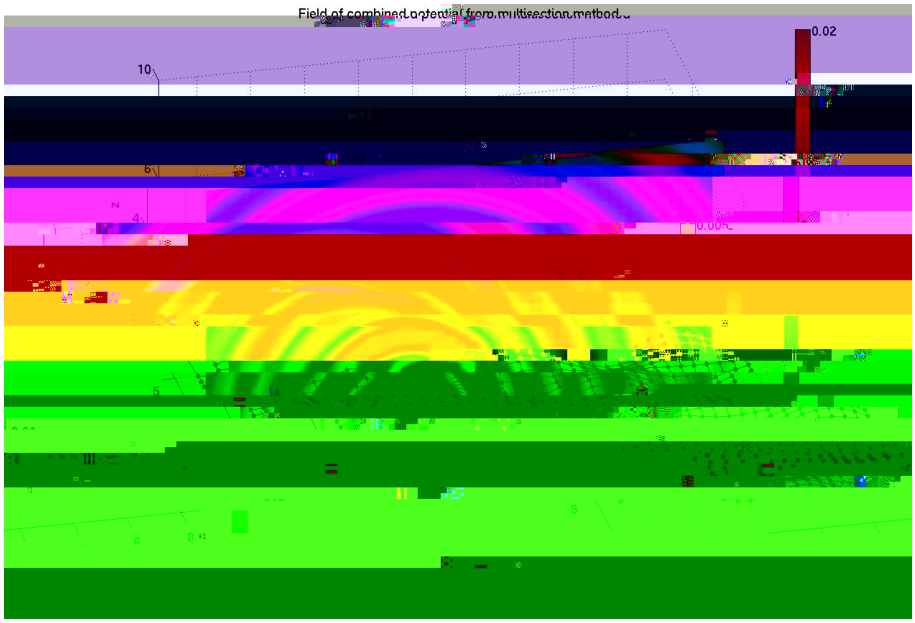
Field of combined potential from multisection method
0.02
10
6
4
5

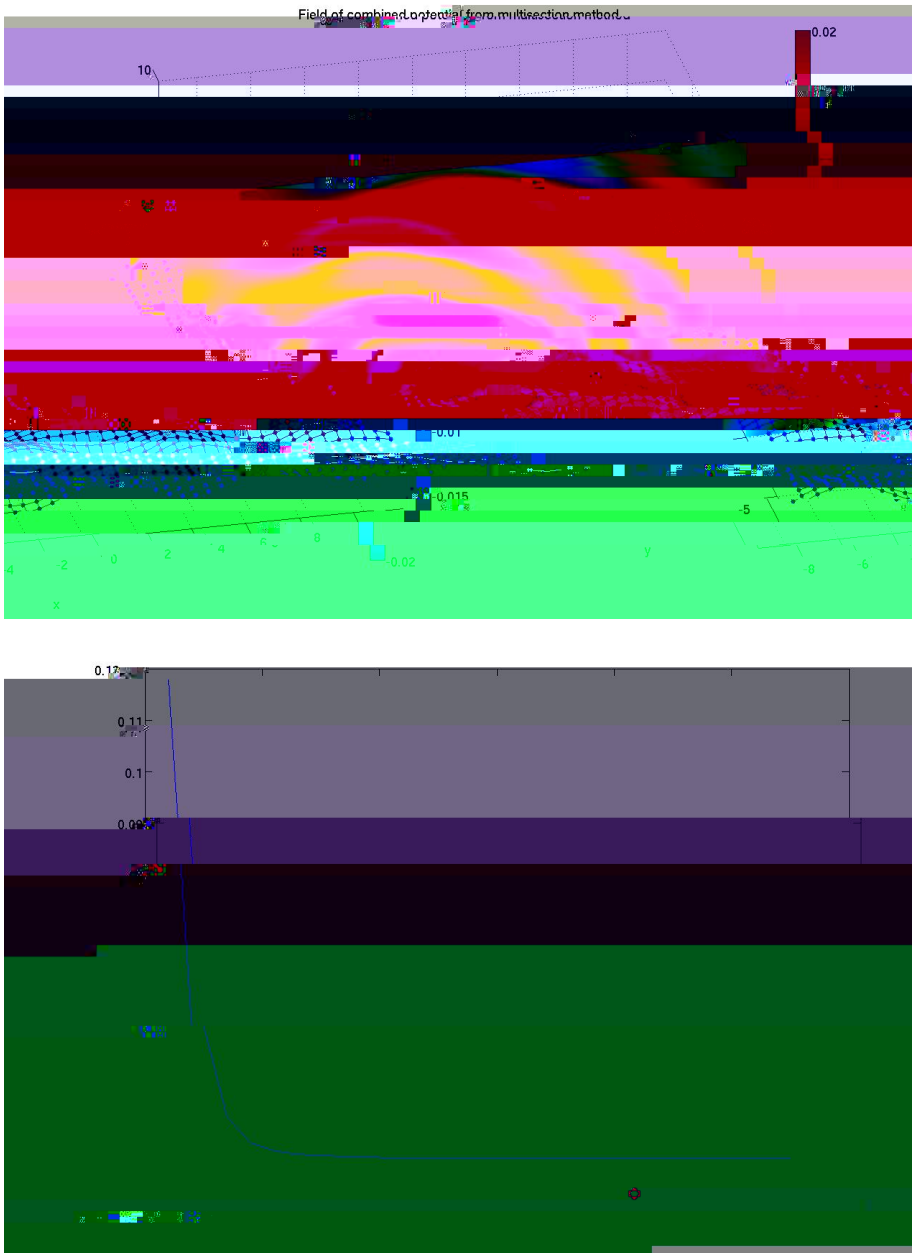

Figure 4: (a) Scattered field for an incident point source with source point $z = (-2, 0, 4)$. (b) Error behaviour for the iterates of the gradient method.

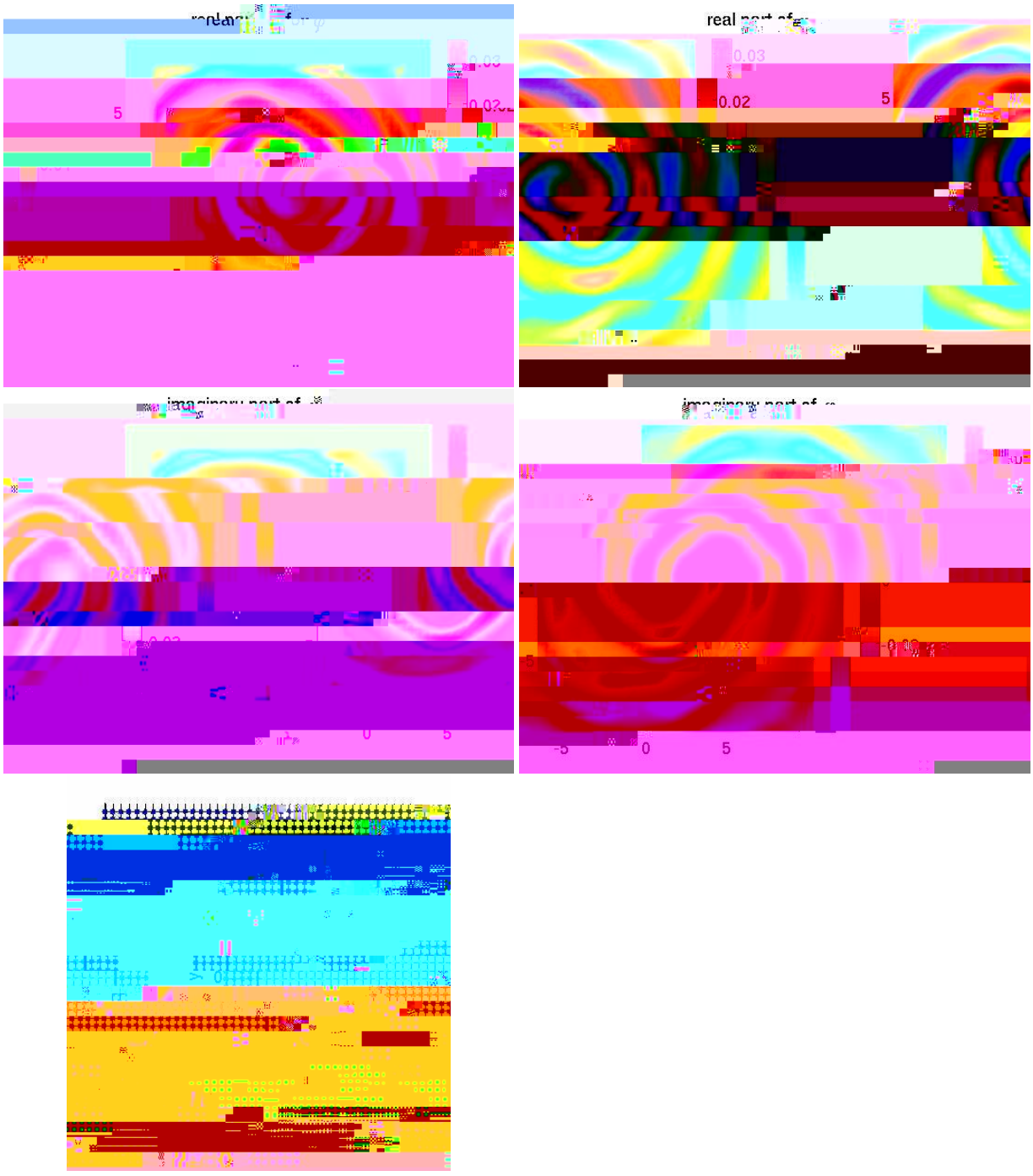

Figure 5: The images show the real and imaginary part of the density ϕ solving the multi-section inequality in the left column and the true density ϕ_0 in the right column. The location of the two di□erent sections B_τ and B is indicated in the image of the third row. On the set B_τ the approximation is good and on $B \setminus B_\tau$ the density ϕ is zero by construction.

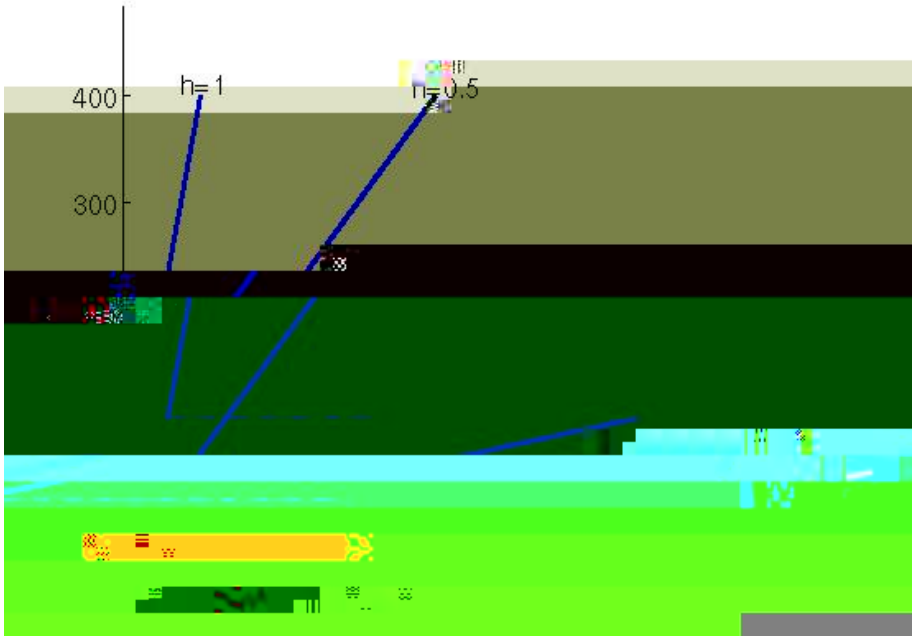

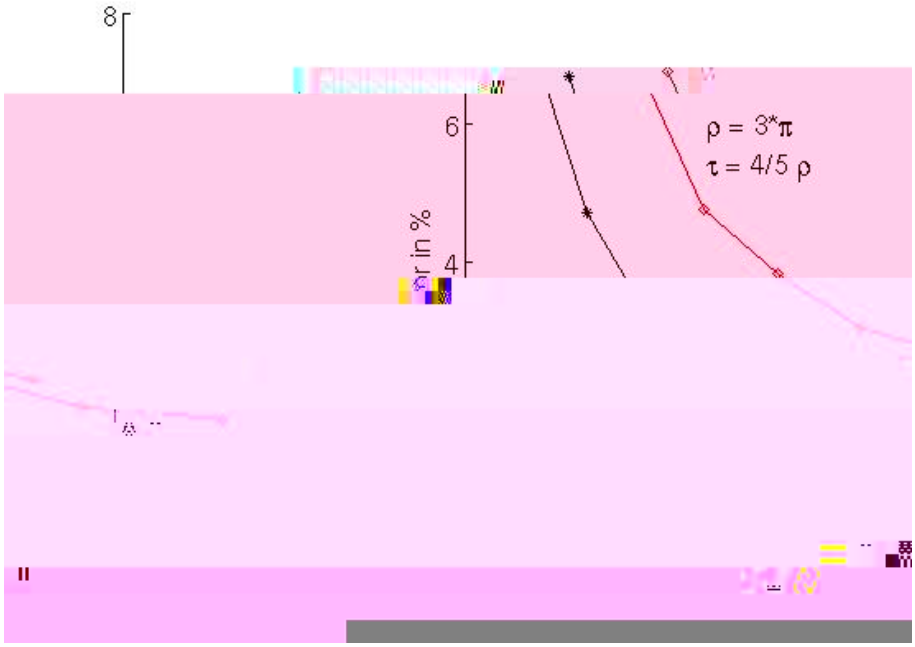

Figure 6: (a) Scheme to discuss the discretization and cut-o error and convergence properties of the multi-section method. (b) Illustration of the relative error measured in the calculated field for di erent choices of cut-o parameters and τ in dependence of the number of unknowns N. In both cases we have chosen a fixed ratio of $\rho/\tau = 4/5$. The black curve with stars shows the error for $\rho = 2\pi$ and the red curve with diamonds shows the error for $\rho = 3\pi$.

References

[1] S. N. Chandler-Wilde, E. Heinemeyer, and R. Potthast. Acoustic scattering by mildly rough unbounded surfaces in three dimensions. *SIAM J. Appl. Math.*, 66:1002–1026, 2006.

[2] S. N. Chandler-Wilde, E. Heinemeyer, and R. Potthast. A well-posed integral equation formulation for three-dimensional rough surface scattering. *Proceedings of the Royal Society of London*, Series A:DOI: 10.1098/rspa.2006.1752, 2006.

[12] M. Saillard and A. Sentenac. Rigorous solutions for electromagnetic scattering from rough surfaces. *Waves Random Media*, 11:R103–R137, 2001.

[13] A. G. Voronovich. *Wave Scattering from Rough Surfaces*. Springer, 1998 2nd Edt.

[14] K. F. Warnick and W. C. Chew. Numerical simulation methods for rough surface scattering. *Waves Random Media*, 11:R1–R30, 2001.